Applied Environmental Research
- RESEARCH FOR SUSTAINABLE PLANET -



Research Article

Kinetics of Hexavalent Chromium Adsorption and Reduction by Living Cells of the Marine Bacterium *Bacillus cereus*

Jittima Charoenpanich*, Wachiraphorn Cherdchoo, Jutamas Pantab, Jariya Supakrit

Department of Biochemistry, Faculty of Science, Burapha University, Bangsaen, Chon Buri 20131, Thailand

*Corresponding Email: jittima@go.buu.ac.th

Abstract

This study identified *Bacillus cereus*, an efficient Cr(VI) bioreducer, isolated from marine sediment in Thailand. Batch experiments verified the complete removal of 25 mg L^{-1} Cr(VI) from synthetic wastewater (pH 7.0) after 6 days at 37 °C, 50 rpm, and a biomass concentration of 25% (v/v) culture inoculum. The Freundlich isotherm model demonstrated the best correlation with the Cr(VI) adsorption equilibrium data in the 25–100 mg L^{-1} concentration range (R^2 = 0.9831). Kinetic analyses indicated that the removal of Cr(VI) by living *B. cereus* followed a pseudo-second-order adsorption model (R^2 = 0.9875) and a pseudo-second-order reduction model (R^2 = 0.9807). The adsorption rate can be accurately characterized via the intraparticle diffusion model and a Boyd plot. This bacterium can remove Cr(VI) in four steps: (1) migration of Cr(VI) from the fluid into the cell membrane; (2) chemical interaction of Cr(VI) with carbon and oxygen functional groups present on the cell surface; (3) multilayer adsorption and diffusion of chromium ions from the cell surface to the internal pores of the cellular particles; and (4) reduction of chromium ions to other forms. This research highlights the potential application of *B. cereus* in mitigating Cr(VI) environmental issues.

ARTICLE HISTORY

Received: 13 Apr. 2025
Accepted: 30 Aug. 2025
Published: 8 Sep. 2025

KEYWORDS

Bioreduction;
Cr(VI) removal;
Bacillus cereus;
Adsorption mechanism

Introduction

Chromium is known as a pollutant that is environmentally persistent and complex. It is predominantly released into the environment via industrial operations. The primary sources of chromium include water discharge resulting from alloy production, leather tanning, and activities within the electronics and metallurgy industries [1]. Chromium occurs naturally at various oxidation levels ranging from −2 to +6. The stable oxidation states of trivalent chromium, Cr(III), and hexavalent chromium, Cr(VI), are the only ones that have significant environmental impacts [2]. As a result, they may display differing behaviors concerning toxicity and mobility. Chromium(III) has relatively low solubility in water, has negligible toxicity [3–4], and functions as an essential trace element for living organisms [5−6]. In contrast, Cr(VI) mostly exists as highly soluble and toxic chromate anions [7], which have been identified in streams on the basis of their origin. Cr(VI) is used in many industries to create a dense, corrosion-resistant, bright finish on metal surfaces in electroplating and as a tanning agent in the leather tanning process. The concentration of Cr(VI) in electroplating effluents ranges from 15 to 30 mg L^{-1}, whereas tannery effluents contain between 1,300 and 2,500 mg L^{-1} Cr(VI) [8]. If improperly handled, Cr(VI) can easily be mobilized and enter the food chain by leaching from landfills and industrial discharges. Chromium (VI) is extremely toxic, mutagenic, carcinogenic, and teratogenic to organisms [9]. Chromium (VI) toxicity in humans includes skin irritation; lung cancer; and harm to the kidneys, liver, and gastrointestinal system [10]. The United States Environmental Protection Agency has established a discharge limit for Cr(VI) at <0.05 mg L^{-1} [11], although total chromium, covering Cr(III), Cr(VI), and its other forms, is regulated at <2 mg L^{-1} [12]. Therefore, to comply with this regulation, chromium-contaminated industrial effluents must be treated before being released into the environment.

A range of physicochemical techniques have been utilized to extract or remove Cr(VI) from industrial

https://doi.org/10.35762/AER.2025030

effluent. These techniques include chemical precipitation, membrane separation, solvent extraction, and ion exchange resins [13−15]. However, these technologies have certain limits, as they require significant energy and financial investments, require large quantities of chemical reagents, or face difficulties in managing the byproducts or secondary wastes generated during the process. Adsorption is an environmentally sustainable method for the elimination of Cr(VI) [16−17]. However, this technique produces significant quantities of chemical sludge, which offers little added value and poses environmental management challenges [18]. Moreover, it is ineffective when faced with low quantities of Cr [19]. Therefore, it is crucial to focus on a cost-effective, practical and eco-friendly feasible strategy.

The transformation of Cr(VI) into other forms with suitable microorganisms presents a highly effective and appealing method for decontamination [20−24]. Compared with traditional methods, this technology offers several benefits, including cost efficiency and the removal of hazardous sludge. A significant amount of research on Cr(VI) removal has focused on the genera *Pseudomonas* [21], *Enterobacter* [22], *Escherichia* [23], and *Bacillus* [24]; however, few reports have focused on marine bacteria, which are well-adapted microorganisms capable of thriving and effectively executing biodegradation processes [25−26]. The mechanisms of reduction are intricate, and the interaction between Cr(VI) and living cells varies among species [27]. Therefore, comprehending the reduction mechanism is essential for effectively overseeing the therapeutic process. Our study investigated a marine bacterium that effectively removes Cr(VI). The optimum conditions for Cr(VI) reduction were examined via a batch bioreactor. The mechanism of Cr(VI) removal by bacteria was anticipated on the basis of the findings from equilibrium isotherms and adsorption kinetics.

Materials and methods

1) Isolation of Cr(VI)-reducing bacteria and strain identification

The bacteria employed in this work were isolated from marine sediments in Koh Jan, Samaesan, Thailand. The physicochemical parameters during collection were 9 m depth, 8.15 mg L^{-1} dissolved oxygen, 2.5% salinity, a seawater temperature of 21 °C, a pH of 7.8, and a pressure of 2.1 atm. The bacterium was isolated in marine broth supplemented with 0.5% (v/v) $K_2Cr_2O_7$ at 37 °C for 72 h. Cultures with growth turbidity were enriched and cultivated 7 times under the same conditions. A portion of the culture (OD600 ~ 0.4) was spread onto marine agar containing 0.5% (v/v) $K_2Cr_2O_7$ and purified by repeated streaking under the same conditions. The isolate that presented the highest growth rate in the presence of 0.5% (v/v) $K_2Cr_2O_7$ was selected and identified according to its biochemical characteristics and 16S rRNA gene sequence [28]. The amplification of the 16S rRNA gene via PCR, sequencing analysis, and phylogenetic tree construction were performed as described previously [29]. The sequencing data were submitted to the GenBank database with the accession number KM370129.

Cr(VI)-reducing bacteria were initially identified by detecting a chromate reductase gene [30]. PCR amplification of the chromate reductase gene was performed via primers derived from the conserved region of the bacterial chromate reductase gene [30]. Chromosomal DNA (250 ng) extracted via a GF-1 nucleic acid extraction kit (Vivantis Technologies Inc., Selangor Darul Ehsan, Malaysia) was used as the DNA template. The PCR procedure commenced with initial denaturation at 95 °C for 5 min, followed by 35 cycles of 1 min at 95 °C, 1 min at 52 °C, and 1 min at 72 °C. The final extension occurred at 72 °C for 7 min. The anticipated PCR product (~300 bp) was purified via a GF-1 Gel DNA Recovery Kit (Vivantis) and subsequently ligated into the pTG19-T vector (Vivantis) following the manufacturer's guidelines. After transformation into *Escherichia coli* DH5α, the plasmids were isolated via a GF-1 Plasmid DNA Extraction Kit (Vivantis). A gene insert was validated, and its similarity was assessed via the Basic Local Alignment Search Tool (BLAST) tool. The synthesis of chromate reductase was then verified via a previously described method [31].

2) Analysis of chromium(VI)

The quantity of residual Cr(VI) was measured via the diphenylcarbazide technique, a colorimetric method used to detect Cr, particularly Cr(VI) [32]. A standard curve for Cr(VI) was established using various concentrations of Cr(VI) ranging from 0 to 2 mg L^{-1}. The R^2 value was 0.9993. Bacterial cells were separated from the culture via centrifugation at 10,000 × g for 10 min, and Cr(VI) levels in the supernatant were quantified. Synthetic wastewater devoid of Cr(VI) served as a control. The proportion of diminished Cr(VI) was computed via Eq.1:

$$\mathrm{Cr(VI)\ reduction\ (\%)} = ((C_i/C_e)/C_i) \times 100 \quad \text{(Eq.1)}$$

where c_i denotes the initial Cr(VI) concentration (mg L^{-1}) and c_e represents the Cr(VI) concentration postreduction (mg L^{-1}). Each experiment was conducted in triplicate, and the results are presented as average values and standard deviations (SDs).

3) Characterization procudures

3.1) Scanning electron microscopy-energy dispersive X-ray (SEM-EDX) analysis

The bacterial cells before and after Cr(VI) adsorption were passed through a 0.2 µm pore nylon membrane filter, rinsed twice with deionized water, and subsequently

fixed in 1% osmium tetroxide in 0.1 M phosphate-buffered saline (pH 7.4) for SEM analysis. The cells were dehydrated in an ethanol series (70–100%), cross-sectioned, and subsequently dried under vacuum. The samples were affixed on an aluminum stub and sputter-coated with gold particles prior to examination via SEM at 15 kV (1450 VP; Leo, Eindhoven, the Netherlands). The analytical parameters were a pressure of 1.3×10^{-2} Pa and a resolution of less than 10 nm. The targeted elements were concurrently examined via EDX (Leo) of the bacterial cells.

3.2) Transmission electron microscopy-energy dispersive X-ray (TEM-EDX) analysis

The bacterial cells were prepared for TEM in the same manner as for SEM. The samples were subsequently isolated via ultrasonic treatment in ethanol, followed by the removal of residual solvents on carbon-coated copper grids. The TEM images were acquired using a JEOL JEM-2100 (JEOL, Peabody, MA, USA) at an accelerating voltage of 200 kV. EDX was conducted using an Oxford PentaFetx5 probe. Cells devoid of Cr(VI) served as a control.

3.3) X-ray photoelectron spectroscopy (XPS) analysis

The bacterial cells were subjected to 50 mg L^{-1} Cr(VI) and incubated for 24 h under optimum conditions for XPS analysis. The cell pellets were subsequently isolated via centrifugation at 10,000 × g at 4 °C for 10 min, rinsed twice with deionized water, and dried at 80 °C for 3 h. Bacterial cells cultivated under analogous conditions devoid of Cr(VI) served as a control. The alterations in the chemical composition of the cells, whether coupled with or without Cr(VI), during the KBr phase were documented via XPS (AXIS ULTRADLD, Kratos Analytical, Manchester, UK). The basal pressure in the XPS analysis chamber was approximately 5×10^{-9} Torr. The materials were stimulated in X-ray hybrid mode using a spot area of 700 × 300 µm and monochromatic Al K_α 1,2 radiation at 1.4 keV. The X-ray anode was operated at 15 kV, 10 mA, and 150 W. The photoelectrons were detected via a hemispherical analyzer positioned at 90° relative to the normal surface of the sample. The spectra were calibrated with VISION II software included with the device, and all the spectra were subjected to charge correction on the basis of the adventitious carbon signal (C1s) at 285 eV and the oxygen signal (O1s) at 533 eV.

4) Adsorption experiments

4.1) Optimization of adsorption conditions

The impact of physical parameters on enhancing the Cr(VI) reduction efficiency of bacteria was initially examined. The experiment was conducted in 50 mL of synthetic wastewater by altering one parameter while keeping the others constant. The synthetic wastewater utilized in this investigation was prepared according to the methods of Pantab et al. [31]. One liter of synthetic wastewater contained sodium acetate (2.56 g), glucose (2.23 g), KH_2PO_4 (43.9 mg), NH_4Cl (229.3 mg), $MgSO_4 \cdot 7H_2O$ (90 mg), and $CaCl_2 \cdot 2H_2O$ (14 mg), and 0.3 mL of trace solution (1 L of trace solution contained $FeCl_3 \cdot 6H_2O$ (1.5 g), H_3BO_3 (0.15 g), $CuSO_4 \cdot 5H_2O$ (0.03 g), KI (0.18 g), and $MnCl_2 \cdot H_2O$ (0.12 g), $Na_2MoO_4 \cdot 2H_2O$ (0.06 g), $ZnSO_4 \cdot 7H_2O$ (0.12 g), $CoCl_2 \cdot 6H_2O$ (0.15 g) and ethylenediaminetetraacetic acid (10 g) were used. The pH of the synthetic wastewater ranged from 6.0–7.0, the total chemical oxygen demand (COD) was 3,040 mg COD L^{-1}, the soluble COD was 2,960 mg COD L^{-1}, the mixed liquor suspended solid (MLSS) concentration was 3.5 mg MLSS L^{-1}, and the ammonia nitrogen (NH_4^+–N) concentration was 34.70 mg N L^{-1}. The parameters examined included culture inoculum (0–45% v/v), solution pH (2.0–12.0), starting Cr(VI) concentration (12.5–100 mg L^{-1}), agitation speed (50–350 rpm at 50 rpm increments), and temperature (20–50 °C at 5 °C increments).

The ultimate reduction of Cr(VI) was examined under the optimal conditions. An acrylic vessel with a capacity of 6 liters (dimensions: height 8 inches × diameter 12 inches) containing 5 liters of synthetic wastewater, first supplemented with a Cr(VI) concentration of 25 mg L^{-1}, was operated continuously for 7 days. The samples were extracted at consistent time intervals and examined for the reduction of Cr(VI) as previously outlined. The bacterial growth was assessed by measuring the optical density at 600 nm. The average values from triple sets are presented with associated errors.

4.2) Optimization isotherms

Adsorption isotherms were determined using 50 mL of synthetic wastewater (pH 7.0) containing Cr(VI) at various starting concentrations (25–100 mg L^{-1}). Experiments were conducted with free *B. cereus* cells at optimum conditions (37 °C and 50 rpm) for 72 h to confirm the attainment of adsorption equilibrium. Each experiment was conducted three times, and the mean values were used for analysis. The equilibrium adsorption capacity of Cr(VI) (mg g^{-1}), denoted as q_e, was determined via Eq.2:

$$q_e = ((C_i - C_e)/m)V \qquad \text{(Eq.2)}$$

where c_i and c_e (mg L^{-1}) represent the initial and equilibrium concentrations of Cr(VI) in the solution, respectively, m signifies the mass of *B. cereus* employed (g), and V denotes the volume of the solution (L).

The Langmuir and Freundlich isotherm models were selectively assessed via experimentally obtained equilibrium data on the basis of the q_e value [33-34].

Langmuir isotherm

The experimental results were analyzed via the Langmuir equation:

$$\frac{c_e}{q_e} = \left(\frac{1}{q_m} c_e\right) + \frac{1}{K_L q_m} \quad \text{(Eq.3)}$$

In this context, "c_e" (mg L^{-1}) denotes the equilibrium concentration of Cr(VI) in solution, "qe" (mg g^{-1}) represents the quantity of Cr(VI) adsorbed at equilibrium, and "q_m" and "K_L" represent the monolayer adsorption capacity (mg g^{-1}) and the Langmuir equilibrium constant (L mg^{-1}), respectively, which elucidates the characteristics of adsorption.

The Langmuir adsorption parameters were ascertained by rearranging the Langmuir equation (Eq. 3) into its linear form as follows:

$$\frac{1}{q_e} = \left(\frac{1}{q_m K_L}\right)\left(\frac{1}{C_e}\right) + \frac{1}{q_m} \quad \text{(Eq.4)}$$

The parameters "q_m" and "K_L" were determined from the plot of $1/q_e$ against $1/c_e$, yielding a linear relationship with a slope of $1/q_m K_L$ and an intercept of $1/q_m$, indicative of full monolayer coverage.

Freundlich isotherm

The Freundlich adsorption equation is expressed in the following general form:

$$q_e = K_f c_e^{\frac{1}{n}} \quad \text{(Eq.5)}$$

In this context, "q_e" and "c_e" retain their definitions from the Langmuir isotherm, whereas "K_f" and "n" are the Freundlich constants that signify the adsorption capacity and intensity, respectively.

The Freundlich equation can be represented in linear form as:

$$\log q_e = \log K_f + \frac{1}{n} \log c_e \quad \text{(Eq.6)}$$

A linear plot of log q_e against log c_e yields a straight line with a slope of 1/n and an intercept of log K_f. The value of 1/n signifies the type of isotherm as follows: 1/n <1 denotes normal adsorption, whereas 1/n >1 suggests cooperative adsorption.

4.3) Adsorption kinetic studies

Kinetic studies were employed to elucidate the mechanism and properties of Cr(VI) adsorption by *B. cereus*. This study evaluated traditional kinetic models predicated on adsorption and reduction to align with the experimental findings. The pseudo-first-order and pseudo-second-order kinetic models [35], along with the intraparticle diffusion model [36] and the Boyd model [37], were evaluated. All the adsorption kinetic tests were conducted at 37 °C at the optimal pH value. Kinetic curves were obtained at specified time intervals of 3 h throughout a duration of 72 h.

Pseudo-first-order kinetic model

A nonlinear variant of the pseudo-first-order kinetic equation is given as:

$$q_t = q_e\left(1 - e^{-kt}\right) \quad \text{(Eq.7)}$$

The linear representation of the pseudo-first-order model is typically articulated as follows:

$$\log(q_e - q_t) = \log q_e - \frac{k_1}{2.303} t \quad \text{(Eq.8)}$$

where "q_e" and "q_t" are the adsorption capacities at equilibrium and at time "t" (min), respectively, measured in (mg g^{-1}), and "k_1" represents the pseudo-first-order rate constant.

The graph of log (q_e-q_t) against time (t) reveals the slope and intercept as k_1 (pseudo-first-order rate constant) and q_e (equilibrium capacity), respectively.

Pseudo-second-order kinetic model

The nonlinear form of the reaction is depicted as follows:

$$q_t = \frac{k_2 q_e^2 t}{1 + k_2 q_e t} \quad \text{(Eq.9)}$$

This represents the integrated rate law for a pseudo-second-order chemisorption reaction, which may be reformulated as:

$$\frac{t}{q_t} = \frac{1}{k_2 q_e^2} + \frac{1}{q_e} t \quad \text{(Eq.10)}$$

In this context, "q_t" (mg g^{-1}) denotes the adsorption capacity at time "t" (min), "q_e" (mg g^{-1}) represents the equilibrium capacity, and "k_2" signifies the pseudo-second-order rate constant.

The graph of $1/q_t$ against t at varying Cr(VI) concentrations yields a linear relationship, characterized by a slope of $1/k_2 q_e^2$ and intercept of $1/q_e$.

Intraparticle diffusion model

This kinetic model is presented as follows:

$$q_t = k_{id} t^{0.5} + \theta \quad \text{(Eq.11)}$$

In this context, "q_t" (mg g^{-1}) represents the quantity of Cr(VI) adsorbed on the surface of the adsorbent at time "t" ($min^{0.5}$), whereas "k_{id}" denotes the intraparticle diffusion rate constant (mg g^{-1} $min^{0.5}$). The parameter θ

is contingent upon film diffusion (external diffusion) in the kinetics of adsorption.

The graph of q_t against $t^{0.5}$ yields a linear relationship. The adsorption process governed by intraparticle diffusion indicates that the intercept θ represents the boundary layer thickness.

Boyd plot

The Boyd plot is depicted as follows:

$$B_t = -0.4977 - \ln(1 - F) \quad \text{(Eq.12)}$$

where "F" represents the fraction of solute adsorbed at time "t" (min), defined as "q_t/q_e", and "B_t" denotes the computed value derived from the equation.

The compatibility of the pseudo-first-order and pseudo-second-order reduction models with the experimental results was also assessed [38]. These methods were utilized to ascertain whether the adsorption mechanism involved "anionic adsorption" or "adsorption-coupled reduction".

Pseudo-first-order reduction:

$$\ln C = \ln C_0 - k_3 t \quad \text{(Eq.13)}$$

Pseudo-second-order reduction:

$$\frac{1}{c} = k_4 t + \frac{1}{c_0} \quad \text{(Eq.14)}$$

where "C_0" and "C" denote Cr(VI) concentrations in solution (mg L^{-1}) at time "0" and "t" respectively, and "k_3" and "k_4" represent the apparent rate constants (min^{-1}).

The optimal alignment of the kinetic models with the experimental data was assessed using the regression coefficient values (R^2) derived from a linear representation of the model equation and Marquardt's present standard deviation (MPSD) established by Marquardt [39–40].

Results and discussion

1) Isolation and identification of Cr(VI)-reducing bacteria

Six bacterial strains were isolated from marine sediments in the Gulf of Thailand. The Cr(VI) reducers were screened by cultivating colonies on marine media supplemented with $K_2Cr_2O_7$ as the chromate source. Among these, one isolate that proliferated on Cr(VI) at a concentration exceeding 25 mg L^{-1}, which is expected to contain chromate reductase [30], was chosen for strain identification. The strain was a rod-shaped, gram-positive bacterium that exhibited a positive catalase reaction. Positive results were observed for the reactions involving glycerol, amygdalin, arbutin, esculin ferric citrate, salicin, and potassium gluconate, whereas negative results were noted for erythritol, methyl-β-D-xylopyranoside, ducitol, inositol, methyl-α-D-mannopyranoside, methyl-α-D-glucopyranoside, inulin, D-melezitose, D-raffinose, xylitol, gentiobiose, D-turanose, D-lyxose, D-tagalose, D- and L-fucose, potassium 2-ketogluconate, and potassium 5-ketogluconate. Fermentation and oxidation were observed for certain substrates (D-ribose, D-glucose, D-fructose, D-mannose, N-acetylglucosamine, D-cellobiose, D-maltose, D-saccharose [sucrose], D-trehalose, amidon [starch], and glycogen), whereas others (D- and L-arabinose, D- and L-xylose, D- and L-arabitol, D-adonitol, D-galactose, L-sorbose, L-rhamnose, D-mannitol, D-sorbitol, D-lactose, and D-melibiose) did not undergo these processes. The bacterium was identified with 99.8% probability as *Bacillus cereus* on the basis of its biochemical properties.

The 16S rRNA gene was sequenced and aligned via the NCBI GenBank and Ez-Taxon databases to verify its identity. A phylogenetic tree was generated via MEGA 6.0 software and the neighbor-joining method (Figure 1). Sequence comparisons indicated that the isolate was classified within the *Bacillus* genus and had the closest phylogenetic relationship to *B. cereus*. This strain presented 99% similarity with the subsequent *B. cereus* strains : *B. cereus* SVK1 (accession no. KF612021), *B. cereus* SBTBC-008 (accession no. KF601957), *B. cereus* L-3 (accession no. KJ572277), and *B. cereus* IHB B 6826 (accession no. KF668460). Consequently, this isolate was unequivocally classified as a novel strain of *B. cereus*.

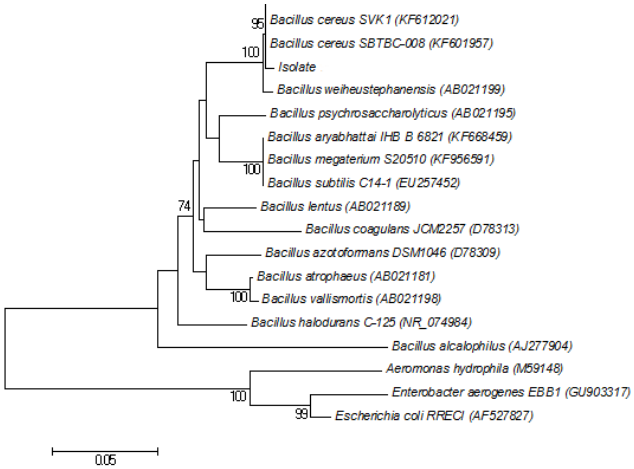


Figure 1 Phylogenetic tree of the isolated *Bacillus cereus*, created via the neighbor-joining algorithm.

The detected *B. cereus* was further examined for the presence of chromate reductase, a crucial enzyme for Cr(VI) reduction [30]. A PCR product of approximately 300 base pairs was cloned and sequenced. BLAST analysis revealed complete sequence identity with the following chromate reductases: chromate reductase, class I flavoprotein chromate reductase of *Escherichia coli* 1303 (accession no. CP009166.1), chromate reductase of *E. coli* BL21DE(3) (accession no. AM946981.2), and

class I chromate reductase YieF of the *E. coli* strain STEC367 (accession no. NZ_CP041429.1). A complete confidence level was demonstrated with the NAD(P)H-dependent chromate oxidoreductase of several *E. coli* strains: *E. coli* strain 14EC047 (accession no. NZ_CP0 24155.1), *E. coli* strain 602354 (accession no. NZ_CP0 25847.1), *E. coli* M8 (accession no. NZ_CP019953.1), *E. coli* strain 120899 (accession no. NZ_CP025916.1), and *E. coli* strain 204446 (accession no. NZ_CP025910.1). The production of chromate reductase was therefore validated via the use of NADH as an electron source [41]. The crude supernatant exhibited an activity of 5.54 ± 0.21 U mL^{-1}. These findings indicate that *B. cereus* may reduce Cr(VI), as chromate reductase was identified.

2) Enhancing the parameters for Cr(VI) reduction

Various parameters were evaluated to identify the most effective circumstances for *B. cereus* to reduce Cr(VI). The culture inoculum was the primary variable assessed for optimization. The findings indicate that growth and Cr(VI) reduction progressively increased with increasing bacterial biomass from 5% (v/v) to 20% (v/v). The removal effectiveness of Cr(VI) increased marginally, attaining a maximum of approximately 74% at a biomass content of 40% (v/v). A minor reduction in Cr(VI) at 45% (v/v) inoculum (69% reduction) likely resulted from mass transfer restrictions. The minimal difference in Cr(VI) reduction percentages between biomass concentrations of 25% (v/v) and 45% (v/v), from 66% reduction to 74% reduction, together with the observed decline in bacterial growth, indicated that the 25% (v/v) culture inoculum was sufficient for Cr(VI) removal and was thus chosen as the optimal dosage for further tests.

The optimal pH range for the reduction of Cr(VI) by most bacterial strains is 6.5–9.0 [42]. Chromate (CrO_4^{2-}) is the predominant Cr(VI) species within this pH range and readily adheres to the positively charged surface through electrostatic interactions [43]. The growth and Cr(VI) reduction of *B. cereus* exhibited comparable patterns and were significantly influenced by the starting pH. The bacterium exhibited no growth in synthetic wastewater at a pH below 5.0. Increasing the pH from 5.0 to 6.0 increased the removal effectiveness from 56.57% to 66.35%. Subsequently, Cr(VI) reduction remained stable (70–75%) with an additional increase in pH from 7.0 to 12.0. A pH of 7.0 was deemed optimal, as the majority of bacteria expend significantly less energy to sustain fundamental processes in neutral environments.

The optimum temperature for *B. cereus* growth was 25 °C, whereas temperatures greater than 40 °C inhibited growth. The proportion of Cr(VI) reduction doubled as the temperature increased from 20 to 30 °C. A significant reduction in efficiency (~75%) was noted at 30–37 °C, which diminished significantly with increasing temperature. The significantly diminished growth and inadequate Cr(VI) reduction at temperatures greater than 40 °C were attributed to the loss of viability or metabolic activity of the bacterial cells during extended incubation. At these temperatures, the functional impairment of reductases, modifications in membrane structure, or changes in ribosomal conformation induce inactivation of the protein synthesis pathway. The reduction in membrane fluidity at low temperatures may impair the operation of transport systems and chromium absorption [44]. This outcome resembled that previously reported for Cr(VI)-reducing bacteria. *B. amyloliquefaciens* [45] and other *Bacillus* species [46] exhibit an ideal temperature of 35 °C for Cr(VI) reduction. Owing to the prevalent use of mesophilic temperatures in bioremediation applications [47], 37 °C was designated the optimal temperature for subsequent investigations.

The growth profile of *B. cereus* exhibited an inverse correlation with the decrease in Cr(VI) concentration across different agitation speeds. Suboptimal cell development at speeds below 150 rpm suggested a constraint in dissolved oxygen, whereas elevated oxygen concentrations promoted bacterial proliferation. The maximum decrease in Cr(VI) (~85%) occurred at 50 rpm. The reduction in efficiency subsequently diminished slightly with increasing agitation speed and remained steady at rates greater than 150 rpm. The decrease in the %Cr(VI) reduction at these agitation speeds may be attributed to foam formation caused by mechanical and/or oxidative stress [48]. Consequently, 50 rpm was identified as the optimal agitation speed for Cr(VI) reduction and was employed in further tests.

The influence of the initial Cr(VI) concentration on bacterial growth and Cr(VI) reduction by *B. cereus* was examined throughout a range of Cr(VI) values from 12.5 to 100 mg L^{-1}. The findings indicated that the reduction efficiency and growth pattern were contingent upon the starting concentration of Cr(VI) employed. A complete decrease in Cr(VI) was achieved, with an initial value of 12.5 mg L^{-1}. A significant reduction in Cr(VI) was observed at concentrations above 25 mg L^{-1}. The reduction efficiency diminished swiftly with increasing starting Cr(VI) concentration. These consequences may result from the toxic and carcinogenic properties of elevated Cr(VI) concentrations, thereby inhibiting growth mechanisms, altering genetic material, and influencing metabolic and physiological responses [49].

3) Continuous operation of Cr(VI) reduction under optimum conditions

The reduction of Cr(VI) by *B. cereus* in synthetic wastewater was conducted continuously for 7 days under optimum conditions (25% [v/v] culture inoculum, 37 °C temperature, pH 7.0, an initial Cr(VI) concentration of 25 mg L^{-1} and an agitation speed of 50 rpm). Cellular proliferation and pH levels were concurrently observed

during the operation. Figure 2 illustrates the findings from a study in which *B. cereus* exhibited slow development, attaining the stationary growth phase after three days. The decrease in Cr(VI) progressively increased during the exponential growth phase. The entire reduction of Cr(VI) was subsequently observed after six days. This can be elucidated by the quorum sensing theory, which posits that when cell densities reach a critical threshold, the expression of inducible genes encoding enzymes pertinent to metabolism is finalized [50]. The minor increase in culture pH may have arisen from the synthesis of $Cr(OH)_3$ during the process [51].

4) Characterization of bacterial cells following Cr(VI) reduction

SEM and TEM examinations were conducted to determine the features of the bacterial cells prior to and following treatment with 25 mg L^{-1} Cr(VI). The SEM image of bacterial cells treated with Cr(VI) revealed a glossy appearance and a coarse surface, in contrast to the untreated cells, which presented flat and smooth surfaces. EDX identified C and O ions as prevalent elements on the surface of *B. cereus* cells (Figure 3a and Figure 3c). The weight proportions of these components decreased following the Cr(VI) treatment, with 3.65 wt% chromium identified (Figure 3b). This study highlights the potential role of carbon and oxygen functional groups in Cr(VI) adsorption. The TEM images confirmed the formation of chromium particles in bacterial cells exposed to Cr(VI). The EDX analysis revealed Cr peaks at 0.04 wt% in Cr(VI)-treated cells (Figure 3d). These findings indicate that Cr(VI) will be converted to other valence states and Cr(III) following its adsorption on the cell surface, which is attributable to a decrease in ambient and internal enzymes. Then, the diminished Cr(III) species readily associate with proteins or engage with nucleic acids [52] and then precipitate within the cells or form complexes with the cell surface. Comparable results were observed for Cr(VI) reduction in other *Bacillus species* [45, 51, 53].

XPS was conducted to determine the chemical alterations on the cell surface of *B. cereus* following cultivation in synthetic wastewater enriched with 25 mg L^{-1} Cr(VI). XPS survey spectra revealed that the bacterial cell surface was predominantly composed of carbon (B.E. = 284.8 eV, C 1 s) and oxygen (B.E. = 531.8 eV, O 1 s). Nevertheless, the spectra revealed no Cr signal following the Cr(VI) treatment. The atomic concentration percentages of carbon and oxygen decreased from 66.38% to 45.08% and from 22.69% to 16.79%, respectively, following Cr(VI) adsorption, indicating that the interaction of Cr(VI) with the bacterial cell surface likely transpired through carbon and oxygen functional groups [54–55]. The increase in the atomic content of potassium from 1.26% to 17.25% signifies cellular adaptability following chromium treatment [56]. The XPS spectra of the C1s and O1s narrow scan regions of the bacterial cell surface, both with and without Cr(VI), were compared. The XPS C1s spectrum of *B. cereus* following exposure to Cr(VI) (Figure 4a) exhibited a displacement in the component peaks associated with graphitic carbon (C-C, B.E. = 285.07 eV, 50%), an ether group (C-O-C, B.E. = 286.49 eV, 28.2%), hydroxy/carbonyl groups (C-O/C=O, B.E. = 288.08 eV, 16.8%), and a carboxy group (O-C=O, B.E. = 289.08 eV, 5.1%). Correspondingly, the XPS O1s spectra (Figure 4b) indicated the participation of carbonyl, hydroxyl, and carboxyl groups in the adsorption and reduction of Cr(VI). The alterations in the peaks indicate that the carbon and oxygen functional groups on the surface of *B. cereus* are linked to Cr(VI) adsorption and reduction.

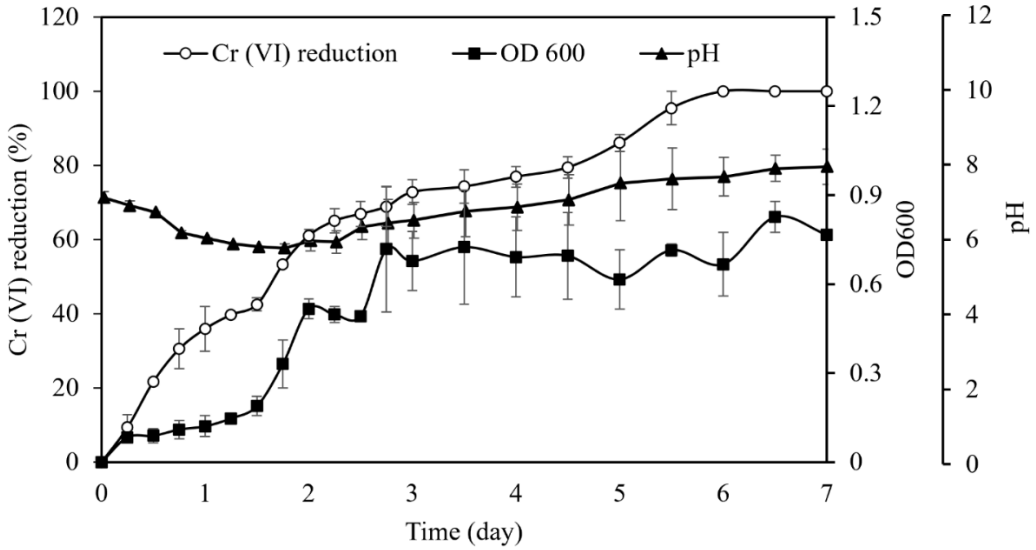


Figure 2 Continuous operation of Cr(VI) reduction by *Bacillus cereus*. Monitoring was conducted in synthetic wastewater under optimum parameters (25% (v/v) culture inoculum, pH 7.0, 25 mg L^{-1} starting Cr(VI) concentration, 37 °C and 50 rpm agitation speed).

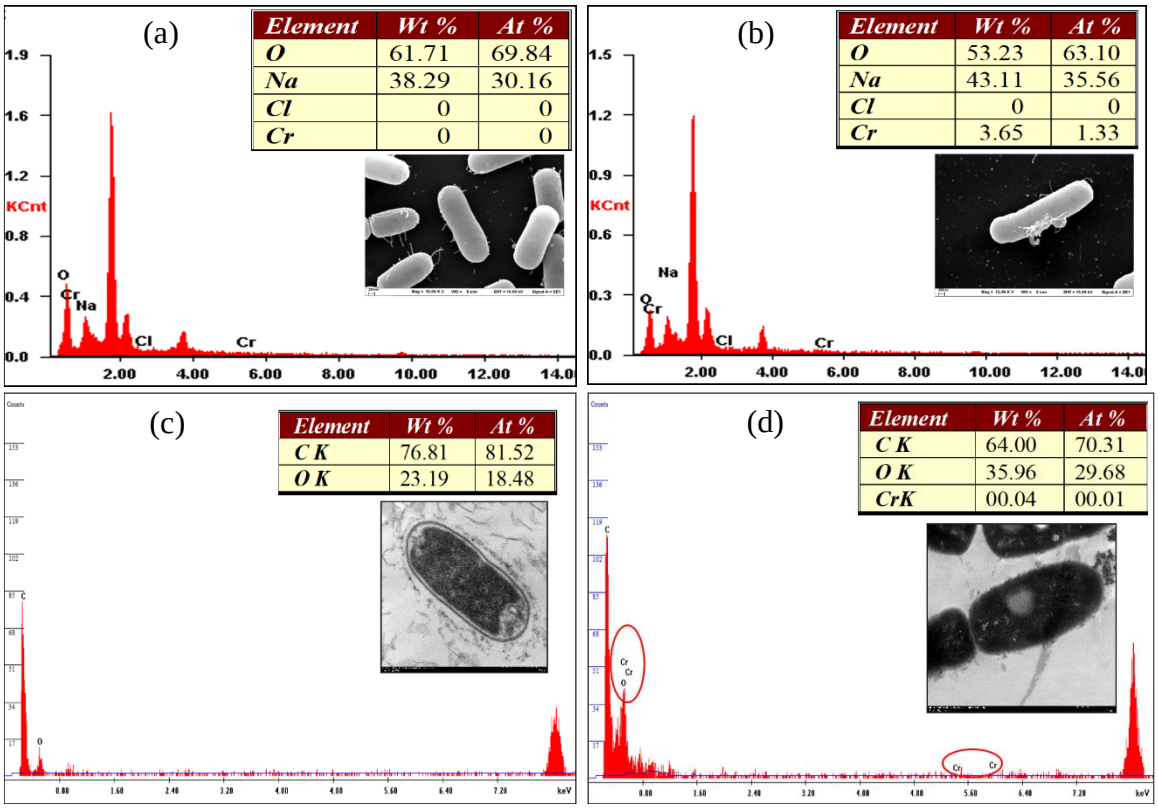


Figure 3 SEM-EDX (a, b) and TEM-EDX (c, d) analyses of *Bacillus cereus* before and after cultivation in synthetic wastewater (pH 7.0) containing 25 mg L^{-1} Cr(VI) at 37 °C and 50 rpm for 24 h.

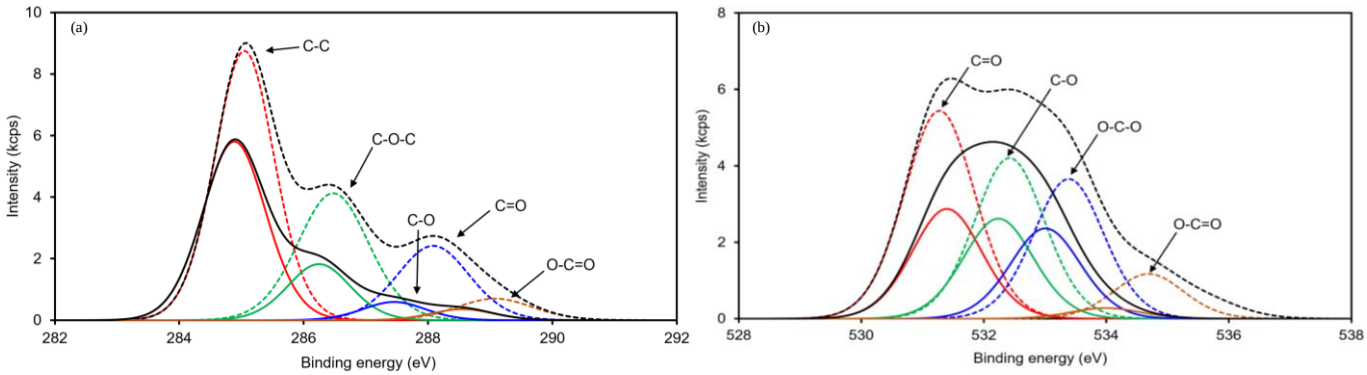


Figure 4 Comparison of X-ray photoelectron spectroscopy (XPS) spectra of *Bacillus cereus* before (dashed lines) and after (solid lines) treatment with Cr(VI). High-resolution (a) C 1 s and (b) O 1 s spectra.

5) Adsorption isotherm and kinetic analyses

The Langmuir and Freundlich isotherm equations were employed to elucidate the mechanism of Cr(VI) adsorption by *B. cereus* at 37 °C. Table 1 presents the experimental data assessed for both models. The maximum adsorption capacity (q_m) was determined to be 16.26 mg g^{-1}, and the K_L value was calculated as 0.3054 L mg^{-1}. The determined R_L values for the adsorption of Cr(VI) on bacterial cells ranged from 0.0317 to 0.1158 L mg^{-1}. This range signifies the advantageous adsorption of Cr(VI) by bacterial cells under experimental conditions. The moderate correlation coefficient (R^2 = 0.936) indicates that the Langmuir isotherm may be inappropriate for Cr(VI) adsorption by this bacterium. The Freundlich isotherm yielded a favorable match for the equilibrium data, with a high R^2 value (R^2 = 0.983). The 1/n value signifies the nature of the adsorption process: 1/n = 0 suggests an irreversible process, 0 < 1/n < 1 denotes an optimal adsorption state, and 1/n > 1 reflects nonoptimal or cooperative adsorption. Our findings indicate that 1/n = 0.31, which is between 0 and 1, indicating advantageous adsorption. The Freundlich isotherm constant (K_f) was determined to be 5.19 mg g^{-1}. A comparative analysis of experimental and calculated adsorption capacity values (Figure 5) demonstrated that the Freundlich isotherm model more accurately represented the adsorption of Cr(VI) onto *B. cereus* than did the Langmuir isotherm model, suggesting that Cr(VI) uptake transpires on heterogeneous surfaces via multilayer adsorption [40].

To better understand the kinetics of Cr(VI) adsorption, the experimental data were evaluated via two adsorption kinetic models: the pseudo-first-order model and the

pseudo-second-order model. Table 2 shows the kinetic constants, correlation coefficients (R^2), and MPSD values that indicate the proximity of the experimental and computed adsorption capabilities. Upon fitting the experimental data to the pseudo-first-order (Figure 6a) and pseudo-second-order kinetic models (Figure 6b), it was determined that the latter more accurately represented the kinetics of Cr(VI) adsorption than did the former. The R^2 value derived from the linear representation of the pseudo-second-order kinetic model (Figure 6e) approached unity (R^2 = 0.9875), surpassing that of the pseudo-first-order model (Figure 6d, R^2 = 0.9570). The adsorption capacities (q_t) derived from the model were comparable to those obtained experimentally. The findings were validated by MPSD values less than 10. The data indicate that the adsorption of Cr(VI) onto the surface of *B. cereus* follows a pseudo-second-order kinetic model. Therefore, it may be inferred that the sorption rate is governed by chemical interactions.

An intraparticle diffusion model was employed to forecast the diffusion mechanism. Figure 6c presents a q_t plot vs. time plot of the diffusion model. The linear segment of the q_t versus $t^{0.5}$ graph (Figure 6f) for the adsorption of Cr(VI) onto bacterial surfaces did not intersect the origin, suggesting that pore diffusion was not the sole rate-controlling mechanism. Three linear segments (R^2 = 0.9765, R^2 = 0.964, and R^2 = 0.9697) were discovered, indicating that the adsorption process adheres to three distinct phases. The k_{id} values (29, 12.405, and 3.712 min^{-1}) for the initial concentration of 25 mg L^{-1} Cr(VI) were derived from the slopes of the corresponding plots at each stage (Table 2). This observation can be ascribed to the adsorption of Cr(VI) due to the boundary layer diffusion effect in the initial phase and the intraparticle diffusion effect in the subsequent two phases.

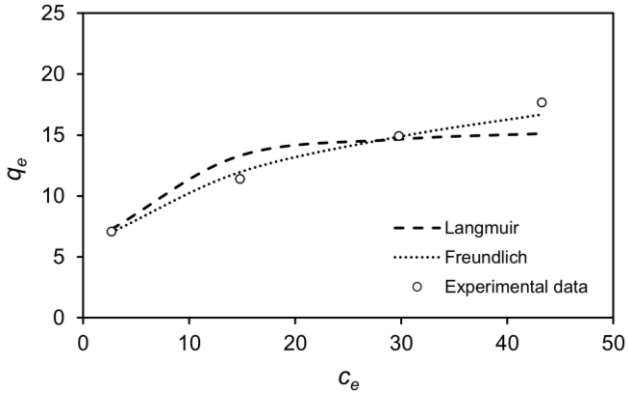


Figure 5 Comparison of the experimental and estimated adsorption capacity values of the Langmuir and Freundlich models for Cr(VI) adsorption by *Bacillus cereus* at concentrations of 25–100 mg L^{-1} Cr(VI). The experimental parameters were as follows: 37 °C, 25% (v/v) culture inoculum, pH 7.0, and 50 rpm.

Table 1 Isotherm parameters for the adsorption of Cr(VI) by *Bacillus cereus*

Langmuir parameters				Freundlich parameters			
K_L (calculated) (L mg^{-1})	R_L (L mg^{-1})	q_m (mg g^{-1})	R^2	K_f (calculated) (mg g^{-1})	1/n	n	R^2
0.3054	0.0317–0.1158 $0 < R_L < 1$	16.26	0.936	5.19	0.31	3.20	0.983

Table 2 Kinetic constants for the removal of Cr(VI) by *Bacillus cereus*

Experimental		Kinetic model constants, R^2 and MPSD							
		Pseudo-first-order adsorption				Pseudo-second-order adsorption			
Cr(VI) (mg L^{-1})	$q_{t,exp}$ (mg g^{-1})	$q_{t,calc}$ (mg g^{-1})	k_1 (min^{-1})	R^2	MPSD	$q_{t,calc}$ (mg g^{-1})	k_2 (min^{-1})	R^2	MPSD
25	149.46	149.21	0.0691	0.9570	15.28	148.94	0.0007	0.9875	8.33
Intraparticle diffusion									
k_{id1} (min^{-1})	θ	R^2	k_{id2} (min^{-1})	θ	R^2	k_{id3} (min^{-1})	θ	R^2	MPSD
29.00	5.42	0.9765	12.405	55.46	0.9640	3.712	118.24	0.9697	6.46
Boyd plot		Pseudo-first-order reduction				Pseudo-second-order reduction			
R^2		k_3 (min^{-1})		R^2		k_4 (min^{-1})		R^2	
0.9693		0.0278		0.9535		0.0044		0.9807	

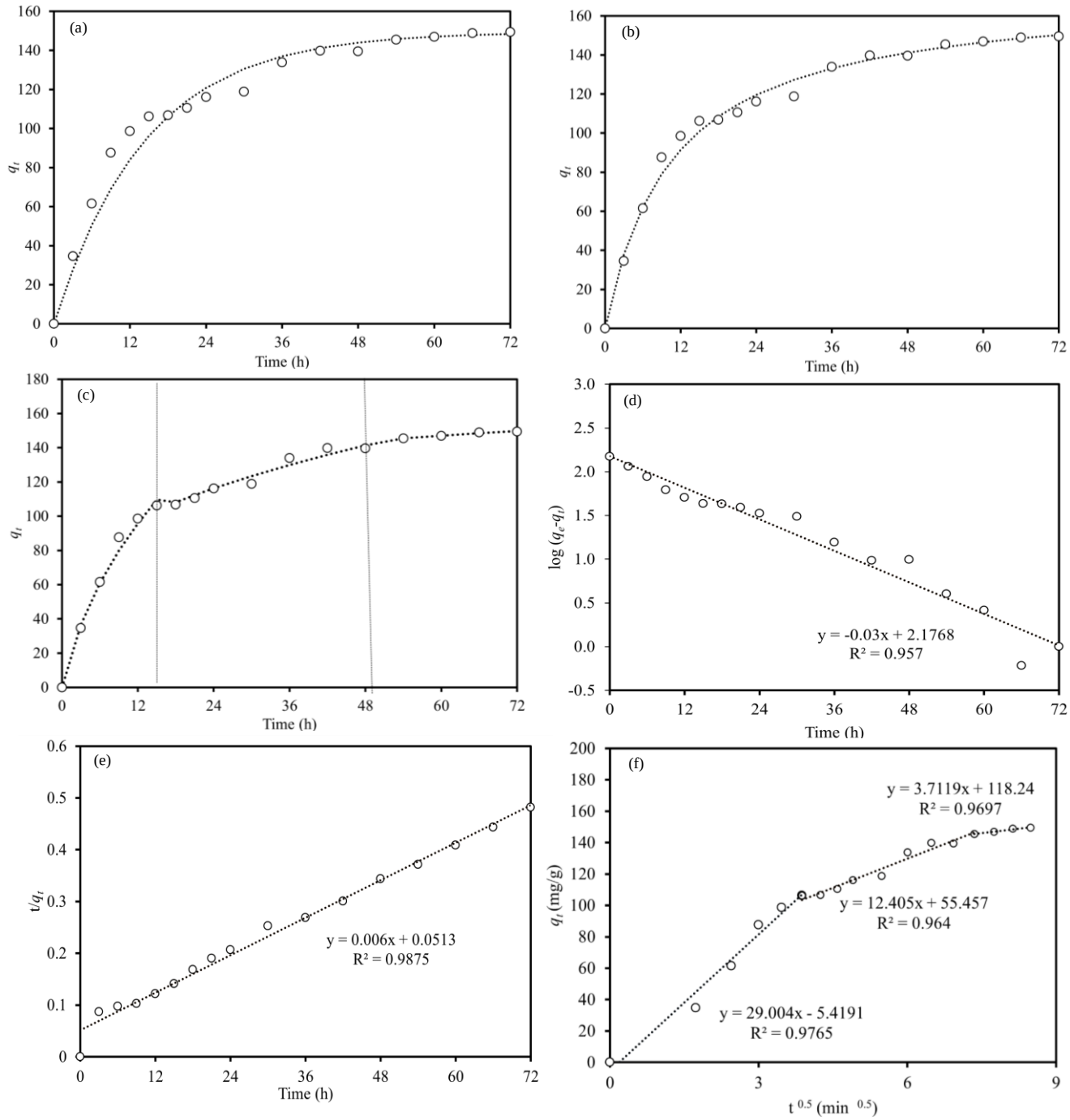


Figure 6 Nonlinear and linear graphs of the adsorption kinetics of Cr(VI) by *Bacillus cereus* at a concentration of 25 mg L^{-1} Cr(VI). (a, d) Pseudo-first-order model; (b, e) pseudo-second-order model; (c, f) intraparticle diffusion model. The symbols denote the experimental data, whereas the dotted lines indicate the theoretical data fitting of the model. The experimental parameters were as follows: pH 7.0, agitation speed at 50 rpm, temperature at 37 °C, and 25% (v/v) culture inoculum.

A Boyd plot was used to predict the rate-limiting stage in the adsorption process. If the plot is linear and intersects the origin, adsorption is governed by particle diffusion; if not, it is regulated by film diffusion [56]. Figure 7 shows a linear curve that does not intersect the origin, indicating that film diffusion governed the adsorption process at the examined concentration. In conjunction with these results, both intraparticle diffusion and film diffusion contribute to the adsorption of Cr(VI) by *B. cereus*.

Two kinetic models predicated on the reduction reaction were employed to correlate the experimental data (Figure 8). The findings indicate that the pseudo-second-order reduction model more accurately represents the experimental data best (R^2 = 0.9807) than does the pseudo-first-order model (R^2 = 0.9535). The reduction of Cr(VI) by *B. cereus* was more accurately represented by this model, suggesting that the removal of Cr(VI) by *B. cereus* primarily involves an adsorption-coupled reduction mechanism rather than biosorption, which necessitates large bacterial surface cells.

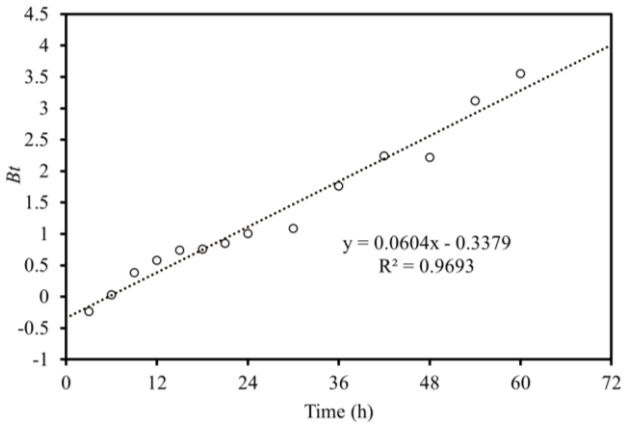


Figure 7 Boyd plot illustrating the removal of Cr(VI) by *Bacillus cereus*. The experimental parameters were as follows: pH 7.0, agitation speed at 50 rpm, temperature at 37 °C, and 25% (v/v) culture inoculum.

A mechanism for Cr(VI) elimination by *B. cereus* can be postulated. Cr(VI) initially migrates from the fluid to the cell membrane. Subsequently, it binds to the cell via chemical interactions, potentially involving the carboxyl, carbonyl, or hydroxyl groups present on the cell surface. Multilayer adsorption on the bacterial cell surface transpires, facilitating the diffusion of chromium ions from the cell surface to the internal pores of the particles. Ultimately, the chromium ions amass within cells and undergo reduction to other forms. While prior research has indicated that *B. cereus* can transform Cr(VI) to Cr(III) and accumulate within the inner portions of bacteria [57–59], the mechanism of Cr(VI) adsorption before reduction is still incomplete. Thus, this paper provides missing information on this adsorption behavior. The total decrease in Cr(VI) and enhanced proliferation in tropical regions, as well as the biosafety level of *B. cereus*, which does not cause disease in healthy humans and poses minimal potential hazard to the environment, indicate the importance of this bacterium for the environmental remediation of Cr(VI), which can easily be disinfected after application.

Conclusions

B. cereus isolated from maritime sand can eliminate Cr(VI) from synthetic wastewater. A complete reduction of 25 mg L^{-1} Cr(VI) was achieved within 6 days at pH 7.0 and 37 °C when the mixture was cultivated with 25% (v/v) culture inoculum with agitation at 50 rpm. SEM-EDX, TEM-EDX and XPS investigations indicated that Cr(VI) was adsorbed onto the bacterial surface via carbon and oxygen functional groups and then taken up by the cell. Adsorption isotherm and kinetic analyses demonstrated multilayer chemisorption on the bacterial cell surface film. The Cr(VI) ions were subsequently internalized into the bacterial cell through pore diffusion and adsorption-mediated reduction processes. This bacterium may have beneficial applications in the biological remediation of Cr(VI)-containing wastewater.

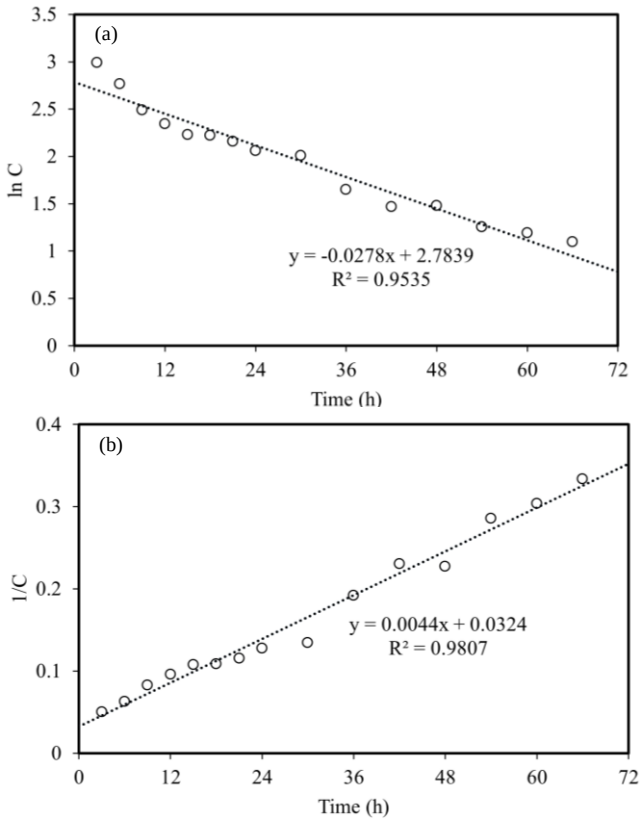


Figure 8 Kinetic study of Cr(VI) reduction by *Bacillus cereus* at a concentration of 25 mg L^{-1} Cr(VI). (a) Pseudo-first-order plot and (b) pseudo-second-order plot. The experimental parameters were as follows: pH 7.0, agitation speed at 50 rpm, temperature at 37 °C, and 25% (v/v) culture inoculum.

References

[1] Mohan, D., Pittman, C.U. Activated carbons and low cost adsorbents for remediation of tri- and hexavalent chromium from water. Journal of Hazardous Materials, 2006, 137, 762–811.

[2] Richard, F.C., Bourg, A.C.M. Aqueous geochemistry of chromium: A review. Water Research, 1991, 25, 807–816.

[3] Lofroth, G., Ames, B.N. Mutagenicity of inorganic compounds in *Salmonella typhimurium*: Arsenic, chromium and selenium. Mutation Research, 1978, 53, 65–66.

[4] Nriagu, J.O., Nieboer, E. Chromium in the natural and human environments. New York: Wiley-Interscience, 1988.

[5] Whitacre, D.M. (Ed) Reviews of environmental contamination and toxicology. Springer, 2013.

[6] Yao, H., Guo, L., Jiang, B.H., Luo, J., Shi, X. Oxidative stress and chromium(VI) carcinogennesis. Journal of Environmental Pathology, Toxicology, and Oncology, 2008, 27, 77–88.

[7] Krishnani, K.K., Ayyappan, S. Heavy metals remediation of water using plants and lignocellulosic agrowaste. Reviews of Environmental Contamination and Toxicology, 2006, 188, 59–84.

[8] Liu, C.C., Wang, M.K., Chiou, C.S., Li, Y.S., Lin, Y.A., Huang, S.S. Chromium removal and sorption mechanism from aqueous solutions by wine processing waste sludge. Industrial and Engineering Chemistry Research, 2006, 45, 8891–8899.

[9] IARC. Monographs on the evaluation of carcinogenic risks to humans: overall evaluation of carcinogenicity. France: An updating of IARC monographs, 1987.

[10] Cieslak-Golonka, M. Toxic and mutagenic effects of chromium (VI): A review. Polyhedron, 1995, 15, 3667–3689.

[11] Chen, J.M., Hao, O.J. Biological removal of aqueous hexavalent chromium. Journal of Chemical Technology and Biotechnology, 1997, 69, 70–76.

[12] WHO. Guidelines for drinking-water quality. 3rd edition. Geneva: World Health Organization, 2004.

[13] Barrera-Díaz, C.E., Lugo-Lugo, V., Bilyeu, B. A review of chemical, electrochemical and biological methods for aqueous Cr(VI) reduction. Journal of Hazardous Materials, 2012, 223, 1–12.

[14] Rengaraj, S., Yeon, K.H., Moon, S.H. Removal of chromium from water and wastewater by ion exchange resins. Journal of Hazardous Materials, 2001, 87, 273–287.

[15] Song, Z., Williams, C.J., Edyvean, R.G.J. Treatment of tannery wastewater by chemical coagulation. Desalination, 2004, 164, 249–259.

[16] Atar, N., Olgun, A., Wang, S. Adsorption of cadmium (II) and zinc(II) on boron enrichment process waste in aqueous solutions: Batch and fixed-bed system studies. Chemical Engineering Journal, 2012, 192, 1–7.

[17] Pintor, A.M.A., Martins, A.G., Souza, R.S., Vilar, V.J.P., Botelho, C.M.S., Boaventura, R.A.R. Treatment of vegetable oil refinery wastewater by sorption of oil and grease onto regranulated cork-A study in batch and continuous mode. Chemical Engineering Journal, 2015, 268, 92–101.

[18] Sharma, I., Goyal, D. Adsorption kinetics: Bioremoval of trivalent chromium from tannery effluent by *Aspergillus* sp. biomass. Research Journal of Environmental Science, 2010, 4, 1–12.

[19] Ahluwalia, S.S., Goyal, D. Microbial and plant derived biomass for removal of heavy metals from wastewater. Bioresource Technology, 2007, 98, 2243–2257.

[20] Thatoi, H., Das, S., Mishra, J., Rath, B.P., Das, N. Bacterial chromate reductase, a potential enzyme for bioremediation of hexavalent chromium: A review. Journal of Environmental Management, 2014, 146, 383–399.

[21] Bopp, L.H., Ehrlich, H.L. Chromate resistance and reduction in *Pseudomonas fluorescens* strain LB300. Archive Microbiology, 1988, 150, 426–431.

[22] Wang, P.-C., Mori, T., Komori, K., Sasatsu, M., Toda, K., Obtake, H. Isolation and characterization of an *Enterobacter cloacae* strain that reduces hexavalent chromium under anaerobic conditions. Applied and Environmental Microbiology, 1989, 55, 1665–1669.

[23] Wang, Y.T., Shen, H. Modelling Cr(VI) reduction by pure bacterial cultures. Water Research, 1997, 31, 727–732.

[24] Garbisu, C., Alkorta, I., Llama, M.J., Serra, J.I. Aerobic chromate reduction by *Bacillus subtilis*. Biodegradation, 1998, 9, 133–141.

[25] Mohapatra, R.K., Pandey, S., Thatoi, H., Panda, C.R. Reduction of chromium (VI) by marine bacterium *Brevibacillus laterosporus* under varying saline and pH conditions. Environmental Engineering Science, 2017, 34 (9), 617–626.

[26] Shi, X.C., Wang, K., Xue, M., Mao, W., Xu, K., Tremblay, P.L., Zhang, T. Ultrafast removal of toxic Cr(VI) by the marine bacterium *Vibrio natriegen*. Chemosphere, 2024, 350, 141177.

[27] Camargo, F.A.O., Bento, F.M., Okeke, B.C., Frankenberger, W.T. Chromate reduction by chromium -resistant bacteria isolated from soils contaminated with dichromate. Journal of Environmental Quality, 2003, 32, 1228–1233.

[28] Weisburg, W.G., Barns, S.M., Pelletier, D.A., Lane, D.J. 16S ribosomal DNA amplification for phylogenetic study. Journal of Bacteriology, 1991, 173, 697–703.

[29] Charoenpanich, J., Soongrung, T., Chinnasri, S., Suebchuea, N., Suppoontong, M., Thiemsawait, S. A novel broad-temperature active and solvent stable esterase from a newly isolated *Bacillus aerophilus*. Biocatalysis and Agricultural Biotechnology, 2018, 13, 116–122.

[30] Patra, R.C., Malik, S., Beer, M., Megharaj, M., Naidu, R. Molecular characterization of chromium (VI) reducing potential in Gram positive bacteria isolated from contaminated sites. Soil Biology and Biochemistry, 2010, 42(10), 1857–1863.

[31] Pantab, J., Sirisom, K., Charoenpanich, J. Adsorption isotherm and kinetic studies of Cr(VI) removal by a new strain of *Staphylococcus sciuri*. ScienceAsia, 2022, 48(5), 605–613.

[32] APHA AWWA. Standard methods for the examination of water and wastewater. Centennial. 25th edition. Washington DC: American Public Health Association, 2005, 1–101.

[33] Freundlich, H.M.F. Over the adsorption in solution. Journal of Physical Chemistry, 1906, 57, 385–471.

[34] Langmuir, I. The evaporation, condensation and reflection of molecules and the mechanism of adsorption. Physical Review, 1916, 8(2), 149–176.

[35] Qiu, H., Lv, L., Pan, B.C., Zhang, Q.J., Zhang, W.M., Zhang, Q.X. Critical review in adsorption

kinetic models. Journal of Zhejiang University-Science A, 2009, 10, 716–724.

[36] Hameed, B.H., Ahmad, A.A. Batch adsorption of methylene blue from aqueous solution by garlic peel, an agricultural waste biomass. Journal of Hazardous Materials, 2009, 164, 870–875.

[37] Boyd, G.E., Adamson, A.W., Myers, Jr L.S. The exchange adsorption of ions from aqueous solutions by organic zeolites, II: kinetics. Journal of the American Chemical Society, 1947, 69, 2836–2848.

[38] Charoenpanich, J., Khotthong, A., Pantab, J., Thasurin, N., Chumjam, S. Adsorption kinetic of *Acinetobacter baylyi* for Cr (VI) removal under acidic condition. Songklanakarin Journal of Science and Technology, 2022, 44(3), 584–593.

[39] Marquardt, D.W. An algorithm for least-squares estimation of nonlinear parameters. SIAM Journal on Applied Mathematics, 1963, 11, 431–441.

[40] Cherdchoo, W., Nithettham, S., Charoenpanich, J. Removal of Cr(VI) from synthetic wastewater by adsorption onto coffee ground and mixed waste tea. Chemosphere, 2019, 221, 758–767.

[41] Sau, G.B., Chatterjee, S., Mukherjee, S.K. Chromate reduction by cell-free extract of *Bacillus firmus* KUCr1. Polish Journal of Microbiology, 2010, 59 (3), 185–190.

[42] Kathiravan, M.N., Karthick, R., Muthu, N., Muthukumar, K., Velan, M. Sonoassisted microbial reduction of chromium. Applied Biochemistry and Biotechnology, 2010, 160(7), 2000–2013.

[43] McLean, J.S., Beveridge, T.J. Chromate reduction by a *Pseudomonad* isolated from a site contaminated with chromate copper arsenate. Applied and Environmental Microbiology, 2001, 67, 1076–1084.

[44] Narayani, M., Shetty, K.V. Chromium-resistant bacteria and their environmental condition for hexavalent chromium removal: A review. Critical Reviews in Environmental Science and Technology, 2013, 43(9), 955–1009.

[45] Das, S., Mishra, J., Das, S.K., Pandey, S., Rao, D.S., Chakraborty, A., …, Thatoi, H. Investigation on mechanism of Cr(VI) reduction and removal by *Bacillus amyloliquefaciens*, a novel chromate tolerant bacterium isolated from chromite mine soil. Chemosphere, 2014, 96, 112–121.

[46] Dhal, B., Thatoi, H., Das, N., Pandey, B.D. Reduction of hexavalent chromium by *Bacillus* sp. isolated from chromite mine soils and characterization of reduced product. Journal of Chemical Technology and Biotechnology, 2010, 85, 1471–1479.

[47] Charoenpanich, J. Removal of acrylamide by microorganisms. *In*: Patil, Y.B., Rao, P. (ed.), Applied bioremediation-active and passive approaches. Croatia: Intech open science online publishers, 2013, 99–119.

[48] Liu, Y.G., Xu, W.H., Zeng, C.M., Tang, C.F., Li, C.F. Experimental study on reduction by *Pseudomonas aeruginosa*. Journal of Environmental Sciences, 2004, 16, 795–801.

[49] Losi, M.E., Frankenberger, W.T. Chromium-resistant microorganisms isolated from evaporation ponds of a metal processing plant. Water Air and Soil Pollution, 1994, 74, 405–413.

[50] Buranasilp, K., Charoenpanich, J. Biodegradation of acrylamide by *Enterobacter aerogenes* isolated from wastewater in Thailand. Journal of Environmental Sciences, 2011, 23 (3), 396–403.

[51] Dadrasnia, A., Wei, K.S.C., Shahsavari, N., Azirun, M.S., Ismail, S. Biosorption potential of *Bacillus salmalaya* strain 139SI for removal of Cr(VI) from aqueous solution. International Journal of Environmental Research and Public Health, 2015, 12 (12), 15321–15338.

[52] Daulton, T.L., Little, B.J., Lowe, K., Jones-Meehan, J. Electron energy loss spectroscopy techniques for the study of microbial chromium (VI) reduction. Journal of Microbiological Methods, 2002, 50, 39–54.

[53] Sukumar, C., Janaki, V., Kamala-Kannan, S., Shanthi, K. Biosorption of chromium (VI) using *Bacillus subtilis* SS-1 isolated from soil samples of electroplating industry. Clean Technologies and Environmental Policy, 2014, 16, 405–413.

[54] Li, X., Cao, J., Zhang, W. Stoichiometry of Cr(VI) immobilization using nanoscale zerovalent iron (nZVI): A study with high-resolution X-ray photoelectron spectroscopy (HR-XPS). Industrial and Engineering Chemistry Research, 2008, 47, 2131–2139.

[55] Sawalha, M.F., Peralta-Videa, J.R., Saupe, G.B., Dokken, K.M., Gardea-Torresdey, J.L. Using FTIR to corroborate the identity of functional groups involved in the binding of Cd and Cr to saltbush (Atriplex canescens) biomass. Chemosphere, 2007, 66, 1424–1430.

[56] Jin, Y., Wang, X., Zang, T., Hu, Y., Hu, X., Ren, G., …, Qu, J. Biosorption of lead (II) by *Arthrobacter* sp. 25: Process optimization and mechanism. Journal of Microbiology and Biotechnology, 2016, 26, 1428–1438.

[57] Rorrer, G.L., Hsien, T. Synthesis of porous-magnetic chitosan beads for removal of cadmium ions from wastewater. Industrial and Engineering Chemistry Research, 1993, 32, 2170–2178.

[58] Chen, Z., Huang, Z., Cheng, Y., Pan, D., Pan, X., Yu, M., …, Wu, Z. Cr(VI) uptake mechanism of *Bacillus cereus*. Chemosphere, 2012, 87, 211–216.

[59] Murugavelh, S., Mohanty, K. Isolation, identification and characterization of Cr(VI) reducing *Bacillus cereus* from chromium contaminated soil. Chemical Engineering Journal, 2013, 230, 1–9.